Journal of Polymer Research (2018) 25: 212
https://doi.org/10.1007/s10965-018-1614-3

ORIGINAL PAPER

Preparation, physicochemical properties and biocompatibility of biodegradable poly(ether-ester-urethane) and chitosan oligosaccharide composites

Na Zhang[1] · Sheng-nan Yin[1] · Zhao-sheng Hou[1] · Wei-wei Xu[1] · Jun Zhang[1] · Ming-hui Xiao[1] · Qi-kun Zhang[1]

Received: 10 January 2018 / Accepted: 4 September 2018 / Published online: 8 September 2018

Abstract

In the paper, novel composites of biodegradable poly(ether-ester-urethane) (PEEU) and water-soluble chitosan oligosaccharide (CHO) were prepared using a simple physical mixing method and their potential application as biomaterials was assessed. The PEEU and CHO were dissolved in *N,N*-dimethylformamide to get a homogenous solution, then the composite films were obtained by the solvent evaporation method. The composites were characterized by FT-IR, and the influence of CHO content on the physicochemical properties of the composite films, including thermal properties, surface morphologies, mechanical properties, surface and bulk hydrophilicity, and in vitro biodegradability, were researched. The thermal stability studies indicated that the composite films had lower initial decomposition temperature and higher maximum decomposition temperature than PEEU film. Only one broad endothermic peak found in DSC curves demonstrated the high compatibility of CHO with PEEU. The ultimate stress and elongation at break of composite films decreased with the increment of CHO content, and the CHO content in the composites should be controlled no more than 25 *wt%* in order to maintain the mechanical properties (ultimate stress: 18.5 MPa; elongation at break: 890%) to meet the requirement of implant materials. The surface morphologies of composite films were observed by cold field emission scanning electron microscope (FE-SEM), and the results indicated that the homogeneous-dispersed composites could be obtained with CHO content being less than 20 *wt%*. The results of water contact angle and water absorption showed that the surface and bulk hydrophilicity were closely related with the water-solubility of CHO component. In vitro degradation studies showed that the degradation rate increased with the increasing content of CHO in composites, indicating that the degradation rate of composite films could be controlled by adjusting CHO content. The surface blood compatibility of the composite films was examined by bovine serum albumin adsorption and platelet adhesion tests. It was found that composite films had improved resistance to protein adsorption and possessed excellent resistance to platelet adhesion.

Keywords Poly(ether-ester-urethane) · Chitosan oligosaccharide · Composites · Physicochemical properties · Biocompatibility

Introduction

Polyurethane (PU) is a synthetic material consisting of repeated blocks of hard and soft segments that provide microphase-separated structure and give the polymer the required elasticity and mechanical strength. Due to the excellent physicmechanical properties and good biocompatibility, PU has been used in many biomedical engineering areas, including blood vessel, cardioids, artificial skins, cartilage, joint and catheter [1–5]. Although PU shows a relatively good biocompatibility compared with other synthetic polymers, blood coagulation is also observed when the PU is used as long-term implanted materials [6]. To further improve their blood compatibility, much attention has been paid to produce a nonspecific protein repelling surface by surface modification methods and creating highly effective non-thrombogenic devices. A preferred strategy is to graft hydrophilic polymers [7, 8] or biomimic materials [9–11] on the surface, thus introducing a high activation barrier to repel proteins.

In recent decades, synthetic/natural polymer blends have received much attention because it is easy and

Na Zhang and Sheng-nan Yin contributed equally to this work.

✉ Zhao-sheng Hou
houzs@sdnu.edu.cn

[1] College of Chemistry, Chemical Engineering and Materials Science, Shandong Normal University, Jinan 250014, People's Republic of China

effective to obtain new materials from the mixing two different polymers. Several studies have prepared and investigated the blends of polyurethane and bioactive nature polymer, and this provides a novel way for modification and exploitation of PU in biomedical application [12–14]. Among the bioactive natural polymer, polysaccharides, which are readily avail-able, inexpensive and biodegradable, appear to be good candidates for use as an additive to improve the blood compatibility of polyurethane matrix.

Chitosan (CH), the linear cationic (1,4)-2-amino-2-deoxy-β-D-glucan produced from chitin by partial deacetylation, is the second most abundant polysaccharide in nature and has been utilized in the biomedical field due to its excellent biocompatibility, antimicrobial activity, and absence of toxicity [15–17]. Nevertheless, its high molecular weight and low solubility in water and organic solvent seriously limited its practical application. Thus, many studies only focus on the blends of PU with superfine CH powder or composites of waterborne PU with CH [18, 19]. As the degradation and deacetylation product of chitin, chitosan oligosaccharide (CHO) consisting of 2–10 glucosamine units bounded via β-1,4-glycoside linkages has attracted more and more attentions recently, because the latter is not only easily soluble in water and in some organic solvent (dimethylsulfoxide and *N,N*-dimethylformamide) due to the shorter chain lengths and free amino groups in D-glucosamine units, but also readily absorbed through the intestine, quickly getting into the blood flow [20, 21]. In addition, CHO, like CH, has positive charges which allow it to bind strongly to negatively charges and possesses distinctive biological activities including antifungal and antibacterial activity, immuno-enhancing effects, antitumor effects and free radical scavenging activity [22–24]. Incorporation of CHO may be very useful in enhancing the biological properties of PU, while few studies about the composites based on PU and CHO were reported.

The purpose of this study was to prepare PU/CHO composites via simple physical mixing for further application in medical field. The biodegradable poly(ether-ester-urethane) (PEEU) with uniform-size hard segments was obtained in our lab [25] and adopted as model PU. The PEEU film exhibited satisfactory mechanical properties and slow in vitro degradation rate, which could meet the requirements of long-term implant materials and made it a good candidate to substitute PU based on aromatic diisocyanate. PEEU and water-soluble CHO were dissolved in *N,N*-dimethylformamide (DMF) to get a homogenous solution, and then the corresponding composite films were obtained by the solvent evaporation method. The influence of CHO content in composites on the physicochemical properties of the films, including thermal properties, surface morphologies, mechanical properties, surface and bulk hydrophilicity, and in vitro biodegradability, were researched. Furthermore, surface blood compatibility of the composite films was examined by protein adsorption and platelet adhesion tests.

Experimental

Materials

Chitosan oligosaccharide (number-average molecular weight of 3000 g/mol, about 90% deacetylated) was purchased from Zhejiang Golden-Shell Biochemical Co., Ltd. (Zhejiang, China). *L*-lactide (*L*-LA) was obtained from J&K Scientific Co., Ltd. and recrystallized three times from dry ethyl acetate. ε-Caprolactone (ε-CL), stannous octoate and hexamethylene diisocyanate (HDI) were purchased from Sigma-Aldrich, and used without further purification except for ε-CL, which was distilled from CaH_2 under reduced pressure. Poly(ethylene glycol) (PEG, $M_n = 600$, Beijing Chemical Reagent Co., Ltd., China) was dried for 4 h at 110 °C under vacuum prior to use. 1,4-Butanediol (BDO, Aladdin Reagent Co. China) was dried over 3-Å molecular sieves and redistilled before use. DMF (AR grade, Aladdin Reagent Co., China) was dried with P_2O_5 and distilled under reduced pressure before use. Phosphate buffer saline (PBS, pH = 7.4) was supplied by Beijing Chemical Reagent Co., Ltd. (China) and used as received. Other reagents were AR grade and purified by standard methods.

Preparation of poly(ether-ester-urethane) (PEEU)

PEEU was prepared according to our previous paper [25]. Briefly, *L*-LA (0.15 mol) was mixed with ε-CL (0.19 mol) in a vacuum flask under nitrogen atmosphere, PEG600 (0.05 mol) and stannous octoate (70 mg) were added as initiator and catalyst, respectively. The mixture was polymerized under reduced pressure at 140 °C for 24 h to give the triblock prepolymer of poly(ε-CL-co-*L*-LA)-PEG-poly(ε-CL-co-*L*-LA) (PCLA-PEG-PCLA). Then, the prepolymer was chain-extended with an isocyanate-terminated urethane (HDI-BDO-HDI) (molar ratio of NCO/OH was 1.05) to obtain the PEEU. The chemical structure of PEEU was shown in Fig. 1, and the molecular weight was measured by gel permeation chromatography (GPC) ($M_w = 149{,}000$, $M_n = 109{,}200$, $M_w/M_n = 1.36$).

Preparation of PEEU/CHO composite films

A typical procedure: A predetermined amount of PEEU and CHO were dissolved in DMF at room temperature under magnetic stirring to get homogeneous solution. Then the solution (4.0 g/100 mL) was poured on to a polytetrafluoroethylene mold. The solvent was removed by natural volatilizing at room temperature for ~6 days and subsequently transferred to

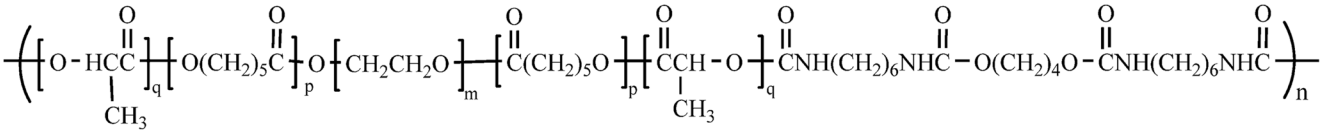

m=13.3; p =2.2; q=3.5

Fig. 1 The chemical structure of PEEU

vacuum drying oven for one day so as to remove the last traces of solvent under reduced pressure. The PEEU/CHO composite films (PUC) were obtained with 0.30 ± 0.02 mm thickness, and the chemical composition of PUC films is listed in Table 1.

Instruments and characterization

Characterization

Fourier transform infrared (FT-IR) spectra were recorded on an Alpha infrared spectrometer (Bruker, Germany) equipped with a Bruker platinum ATR accessory at room temperature using film (composites) or powder (CHO) as samples. Each sample was scanned from 4000 to 400 cm^{-1} with resolution of 4 cm^{-1}. The number/weight-average molecular weight (M_n, M_w) and polydispersity index (M_w/M_n) of PEEU were obtained using a TriSEC302 (Viscotec, USA) gel permeation chromatography (GPC) at 25 °C. The eluting solvent was tetrahydrofuran (THF) at a flow rate of 1.0 mL/min. The retention times were calibrated against five known narrow polydispersity polystyrene standards.

Thermal properties

The thermal transition behavior was determined by differential scanning calorimeter (DSC) (DSC2910, Universal, USA). The samples were sealed in aluminum pans and scanned from −70 °C to 150 °C with a heating rate of 10 °C/min under a continuous nitrogen purge (30 mL/min). Thermogravimetric analysis (TGA) was performed using a TGA 2050 analyzer (Universal, USA), and the samples were performed from 50 to 600 °C at a heating rate of 20 °C/min^{-1} under nitrogen atmosphere with a gas flow rate of 50 mL/min^{-1}.

Mechanical properties

Stress-strain properties of the composite films were determined on a single-column tensile test machine (Model HY939C, Dongguan Hengyu Instruments, Ltd., China). Dumbbell-shaped specimens were prepared from the films with a punching die of 12 mm width and 75 mm length, the neck width and length were 4.0 and 30 mm, respectively. The test procedure was carried out at a cross-head speed of 50 mm/min at room temperature. Five tensile specimens were tested, and the results were averaged.

Water contact angle

The surface hydrophilicity of the films was measured by contact angle measurement. The sessile static water contact angle was performed by a drop shape analysis system (CAM 200, KSV Instruments, Finland) using a sessile drop technique with ultrapure water as test fluid at room temperature. A minimum of six measurements on at least three different surfaces were measured for each composite film.

Water absorption

The bulk hydrophilicity (swelling property) of the films was quantified by measuring the water absorption content [26, 27]. The dried and weighed film discs (m_d) with ~10.0 mm diameter were incubated in deionized water at 37 ± 0.1 °C for 24 h to reach the water absorption equilibrium. And then, the swollen samples were removed and gently blotted with filter papers to remove adsorbed water and weighed immediately (m_w). The water absorption was calculated according to the equation: Water absorption (%) = $(m_w - m_d)/m_d \times 100$. At least five samples were tested for each film.

In vitro *degradation*

In vitro degradation of films was assessed through the weight loss in PBS (pH = 7.4). Each film discs (~10.0 mm diameter) were placed into an individual sealed bottle containing 10 mL PBS, and incubated in a biochemical incubator at 37 ± 0.1 °C. At selected time intervals, the samples were taken out, washed

Table 1 The chemical composition of PUC films

Films Components	PUC-0	PUC-5	PUC-10	PUC-15	PUC-20	PUC-25	PUC-30	PUC-35
PEEU /g	4.0	3.8	3.6	3.4	3.2	3.0	2.8	2.6
CHO /g	0	0.2	0.4	0.6	0.8	1.0	1.2	1.4
CHO content /*wt%*	0	5	10	15	20	25	30	35

with distilled water, and vacuum dried at room temperature until constant weight. The weight loss could be calculated by comparing the rest weight (W_r) of the discs after degradation for a predetermined time with the original weight (W_o): Weight loss (%) = $(W_o - W_r)/W_o \times 100$. The measurements were performed for 60 days or until the loss of integrity of the films, and the results were the average of three tests.

Surface morphologies

The samples of composite films and PUC-15 after degradation for fixed time were collected to observe the surface morphologies. The dried samples were mounted on aluminum stubs with conductive graphite-filled tapes and sputter-coated with a gold layer under vacuum. Film surface morphologies were observed by a cold field emission scanning electron microscope (FE-SEM, Hitachi SU8010, Japan).

Protein adsorption

The amounts of albumin adsorbed onto the surface were quantified using a Bradford protein assay with bovine serum albumin (BSA) as the model protein [28, 29]. After being equilibrated with PBS (pH = 7.4) for 12 h to achieve complete hydration, the film discs were immersed in 1.0 mL BSA solution (45 μg/mL, the same as the concentration of normal plasma) and incubated for 180 min at 37 ± 0.5 °C. The discs were removed from the solution and then rinsed with fresh PBS three times to remove the unbound BSA. The adsorbed protein on the surface was detached by sonication in 1 *wt*% of sodium dodecylsulfonate aqueous solutions for 30 min. The concentrations of the adsorbed BSA were determined using a micro-Bradford protein assay kit (Sangon Biotech Co., Ltd., Shanghai) with a multiwell microplate reader (Multiskan Mk3-Thermolabsystems, Thermo Fisher Scientific, Inc., USA) at 595 nm. The amount of the adsorbed protein was calculated from the standard curve of optical density against BSA concentration. Independent measurements were performed in triplicate samples and values relative to the control (PBS solution) were reported.

Platelet adhesion

The interactions between the blood and films were assayed by platelet adhesion experiment. The fresh rabbit blood containing sodium citrate as an anticoagulant (Shandong Success Pharmaceutical Technology Co., Ltd., China) was centrifuged at 2000 rpm for 20 min at 4 °C to obtain platelet-rich plasma (PRP). After being equilibrated with PBS for 2 h, the film discs were taken out and incubated with 1.0 mL PRP at 37 °C for 60 min. The discs were rinsed with fresh PBS for three times by mild shaking to remove non-adherent platelets. Adhered platelets were fixed with 2.5% glutaraldehyde for 30 min at room temperature. And then, the films were dehydrated by systemic immersion in a series of ethanol-water solutions [50, 60, 70, 80, 90, 100% (*v/v*)] for 20 min in each step and dried under vacuum. Finally, the platelet-attached surfaces were examined by FE-SEM after coating with gold.

Results and discussion

FT-IR

The composite materials were characterized by FT-IR, and the spectra of CHO powder and composite films with different CHO content are shown in Fig. 2. In the spectrum of CHO (Fig. 2a), the absorption bands at 3400 cm^{-1}, 2872 cm^{-1} and 1023 cm^{-1} were attributed to the characteristic stretching frequencies of -OH, -CH_2- and cyclic ether C-O-C, respectively; the weak absorption bands observed at 1658 and 1574 cm^{-1} belonged to the characteristic absorption peaks of amide I and amide II, which was attributed to the residual amide linkage in CHO. In the spectrum of pure polyurethane (PUC-0, Fig. 2b), the absorption bands at 3321, 1731, 1683, 1529 cm^{-1} were attributed to the characteristic stretching frequencies of N-H, ester C=O, amide I and amide II, respectively; the broad intense bands at 1089 and 1037 cm^{-1} belonged to ester bonds C-O-C and ether bonds C-O-C stretching vibration, respectively.

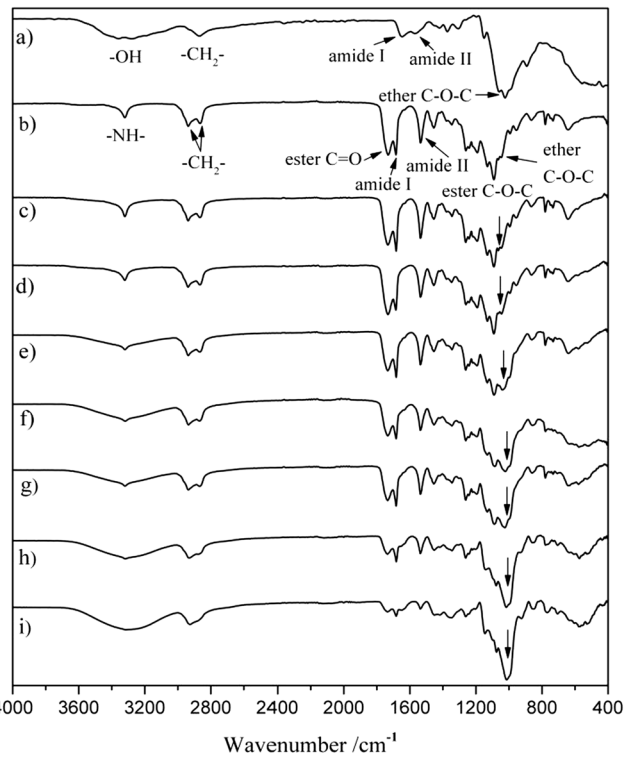

Fig. 2 FT-IR spectra of **a**) CHO powder, **b)** PUC-0, **c)** PUC-5, **d)** PUC-10, **e)** PUC-15, **f)** PUC-20, **g)** PUC-25, **h**) PUC-30, and **i**) PUC-35 films

All the characteristic absorption of CHO and polyurethane were observed in FT-IR spectrum of PUC (Fig. 2c). Moreover, with the increment of CHO content in PUC (Fig. 2c–i), the absorption intensity of cyclic ether C-O-C at ~1574 cm^{-1} increased and ester C=O at ~1731 cm^{-1} decreased. In addition, the relative intensity of amide I (~1680 cm^{-1}) increased slightly compared with that of ester C=O, which should be attributed to the residual amide linkage in CHO (90% deacetylated) [30]. As the paper reported [31], new hydrogen bonds could be formed between chitosan and polyurethane. Thus, it can be deduced that there are existing strong inter-chain interactions between CHO and PEEU in the composites.

Thermal transition

The thermal transition of the composites with different compositions, including glass-transition temperature (T_g), crystallization and melting behaviors, were initially studied by DSC. The DSC thermograms of the CHO powder and representative composite films are presented in Fig. 3. In the DSC curve of CHO (Fig. 3a), no obvious T_g was observed, which should be due to the low molecular weight (~3000 g/mol). And a broad melting endothermic peak was appeared at 35~140 °C with melting enthalpy of 41 J/g, which may due to the vaporization of the water in CHO (the water was very hard to be removed even after the CHO was dried in vacuum), indicating its hygroscopic nature. The T_g was found at lower temperature of −36 °C in the DSC curve of pure polyurethane (PUC-0, Fig. 3b), which was attributed to the soft segments in polyurethanes. The broad endothermic peak at higher temperature of 29~82 °C melting enthalpy of 12 J/g should be due to the melt of hard domains, and the small melting enthalpy indicated that the crystallinity of PUC-0 was low. In the DSC curves of PUC films with different CHO content (Fig. 3c–e), the T_g was observed at almost the same temperature as that of polyurethane (PUC-0). Only one endothermic peak with broader temperature was found (PUC-10: 28–104 °C; PUC-20: 29–126 °C; PUC-30: 26–136 °C) with melting enthalpy from 18 to 37 J/g indicated the high compatibility of CHO with polyurethane (especially with the hard segments of PEEU, because the polarity of CHO was similar with that of hard segments of PEEU).

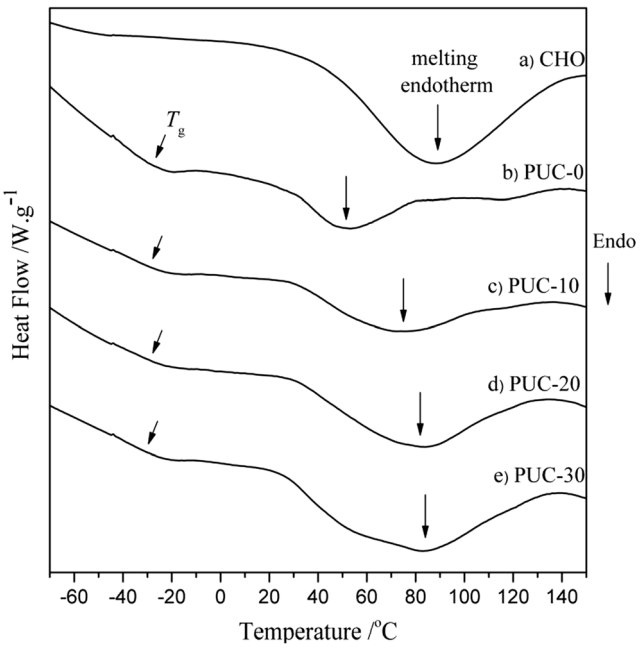

Fig. 3 DSC thermograms of CHO powder and representative composite films (PUC-0, PUC-10, PUC-20, and PUC-30)

Thermal stability

The TGA analyses of the CHO powder and composite films with different CHO content are shown in Fig. 4. Two decompositions occurred in curve of CHO, the first decomposition happened in the temperature ranging from room temperature to 100 °C which was attributed to the water loss in CHO; while the second decomposition began at 200 °C which resulted from the decomposition of the sample itself, and the remaining weight was ~38 wt% at 600 °C. The similar results were found in TGA curves of quaternized carboxymethyl CHO [32]. Pure polyurethane film (PUC-0) exhibited an initial decomposition temperature at about 280 °C with negligible weight loss from about 420 to 600 °C, and the remaining weight was lower than 2 *wt%*. From the TGA curves of composite films, it could be seen that with the CHO content in PUC increasing from 5 to 35 *wt%*, the initial decomposition temperature decreased from 220 to 120 °C, while the maximum decomposition temperature became higher and higher, which was consistent with the higher thermal stable of CHO than that of polyurethane at high temperature. Only one-step decomposition

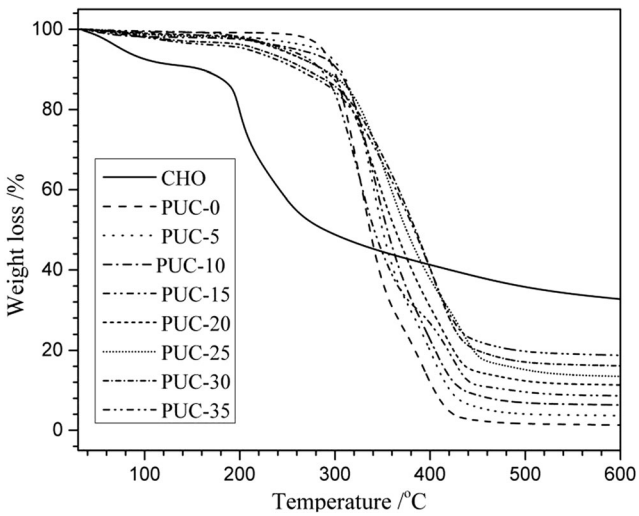

Fig. 4 TGA curves of CHO powder and composite films with different CHO content

found in the curves of PUC indicated that the CHO component was compatible with polyurethane component.

Mechanical properties

The typical stress-strain behaviors of the composite films with CHO content from 0 *wt%* to 35 *wt%* are presented in Fig. 5, and the characteristic values derived from these curves are shown in Table 2. The stress-strain behaviors of composite films displayed a pronounced yield point and behaved as the normal elastomers, showing a smooth transition from elastic to plastic deformation regions [33]. The pure polyurethane film (PUC-0) with uniform-size hard segments had good mechanical properties with ultimate stress of 27.0 MPa, elongation at break of 1210% and initial modulus of 19.9 MPa, while the film of pure CHO was too brittle to be obtained because of the low molecular weight. When the CHO was blended in PEEU, both ultimate stress and elongation at break decreased, which was not in agreement with the previous study about the composite film of water-borne PU (WPU) and CH [19]: the elongation at break decreased and the ultimate stress increased with the increment of CH content. Because the molecular weight of CHO (~3000 g/mol) is much lower than that of CH (200,000~400,000 g/mol), the CHO exhibits almost no mechanical properties. When the content of CHO increased from 5 to 25 *wt%*, the ultimate stress and elongation at break decreased gradually to 18.5 MPa and 890%. However, the ultimate stress and elongation at break decreased relatively sharply when the amount of CHO content increased to an amount over 25 *wt%* (PUC-30 and PUC-35). As a result, the CHO content in the composites should be controlled no more than 25 *wt%* in order to maintain the mechanical properties to meet the requirement of biomaterials. With the increment of CHO content, the initial modulus of the composite films first increased and then decreased, which could be related with the hydrogen bonds between PEEU and CHO. At an appropriate content of CHO in PUC (PUC-15), more hydrogen bonds were formed, resulting in higher initial modulus (Table 2).

Table 2 Mechanical properties of composite films with different CHO content

Films	Elongation at break (%)	Ultimate stress (MPa)	Yield stress (MPa)	Yield strain (%)	Initial modulus (MPa)
PUC-0	1210 ± 17	26.9 ± 2.2	19.2 ± 1.6	96.5 ± 3.5	19.9
PUC-5	1130 ± 15	24.6 ± 1.8	13.4 ± 1.2	73.7 ± 2.6	18.2
PUC-10	1056 ± 15	23.5 ± 1.6	11.9 ± 1.1	53.9 ± 2.1	22.1
PUC-15	996 ± 13	22.3 ± 1.6	15.2 ± 1.4	45.1 ± 1.8	33.7
PUC-20	942 ± 11	20.1 ± 1.5	13.1 ± 1.3	52.8 ± 1.75	24.8
PUC-25	890 ± 11	18.5 ± 1.3	12.9 ± 1.0	50.3 ± 1.55	25.6
PUC-30	789 ± 8	15.1 ± 0.9	10.3 ± 0.7	80.5 ± 2.2	12.7
PUC-35	655 ± 7	12.0 ± 1.0	6.8 ± 0.3	57.8 ± 1.6	11.7

Surface and bulk hydrophilicity

The surface and bulk hydrophilicity of biomaterials are important parameters in many medical applications. The surface and bulk hydrophilicity of the composite films with different CHO content were evaluated by measuring the contact angle formed between water drops and surface of the films (Fig. 6) and the amount of water that each film absorbed (Fig. 7), respectively. As shown in Fig. 6, there was a remarkable difference in contact angle between different CHO content in composite films. Pure polyurethane film (PUC-0) showed characteristically high water contact angle of 97°, indicating that the film had a hydrophobic surface. When the CHO content increased from 5 to 35 *wt%*, the surface hydrophilicity increased gradually with the

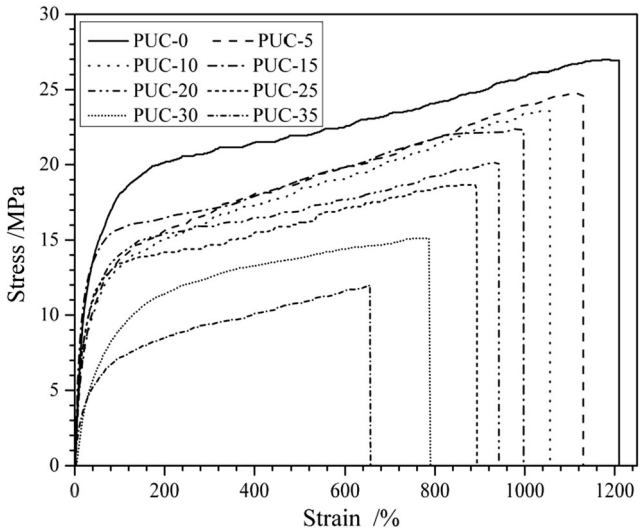

Fig. 5 Typical stress-strain behaviors of composite films with different CHO content

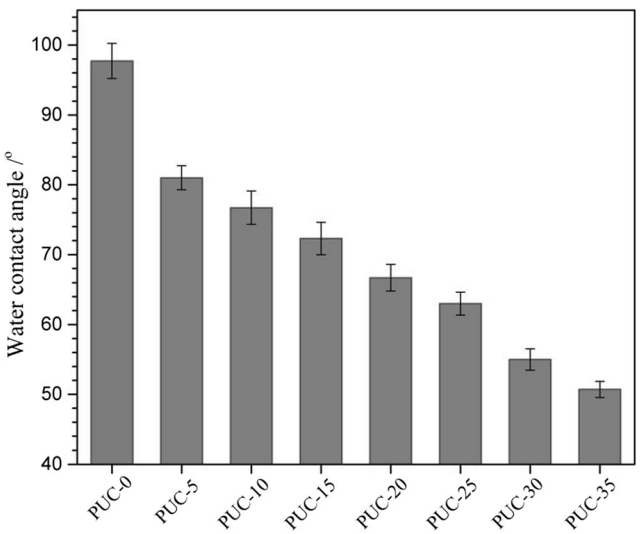

Fig. 6 Data of water contact angle on the surfaces of composite films with different CHO content

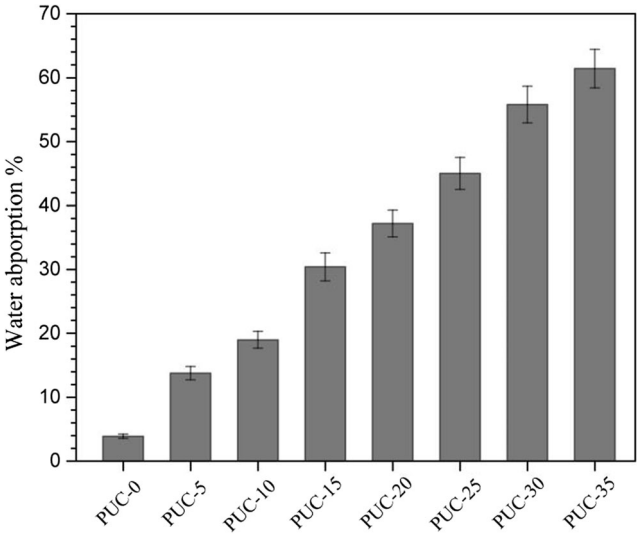

Fig. 7 Data of water absorption of composite films with different CHO content

water contact angle decreasing from 81 to 57.1°, which was ascribed to the introduction of hydrophilic amino groups and hydroxyl groups in CHO. The result was opposite with that of WPU/CH composites, because CH had high crystallinity and the rigid chain hindered the polar groups to come to the polymer surface [19]. The water absorption of the composite films increased gradually from 3.9 to 61.4 *wt%* with CHO content increasing from 0 to 35 *wt%* (Fig. 7), which was also attributed to the hydrophilicity of CHO. From the results of water contact angle and water absorption, the ability of surface and bulk hydrophilicity, which plays an important role in the degradation rate during hydrolytic degradation, is mainly affected by the content of hydrophilic CHO in composites. Hence, the degradation rate of the composite films may be controlled by adjusting the CHO content in composites.

Surface morphologies

Surface morphologies can directly reflect the dispersion homogeneity. The upper surface of the dried composite films with different CHO content were observed with FE-SEM, and the representative micrographs are shown in Fig. 8. The

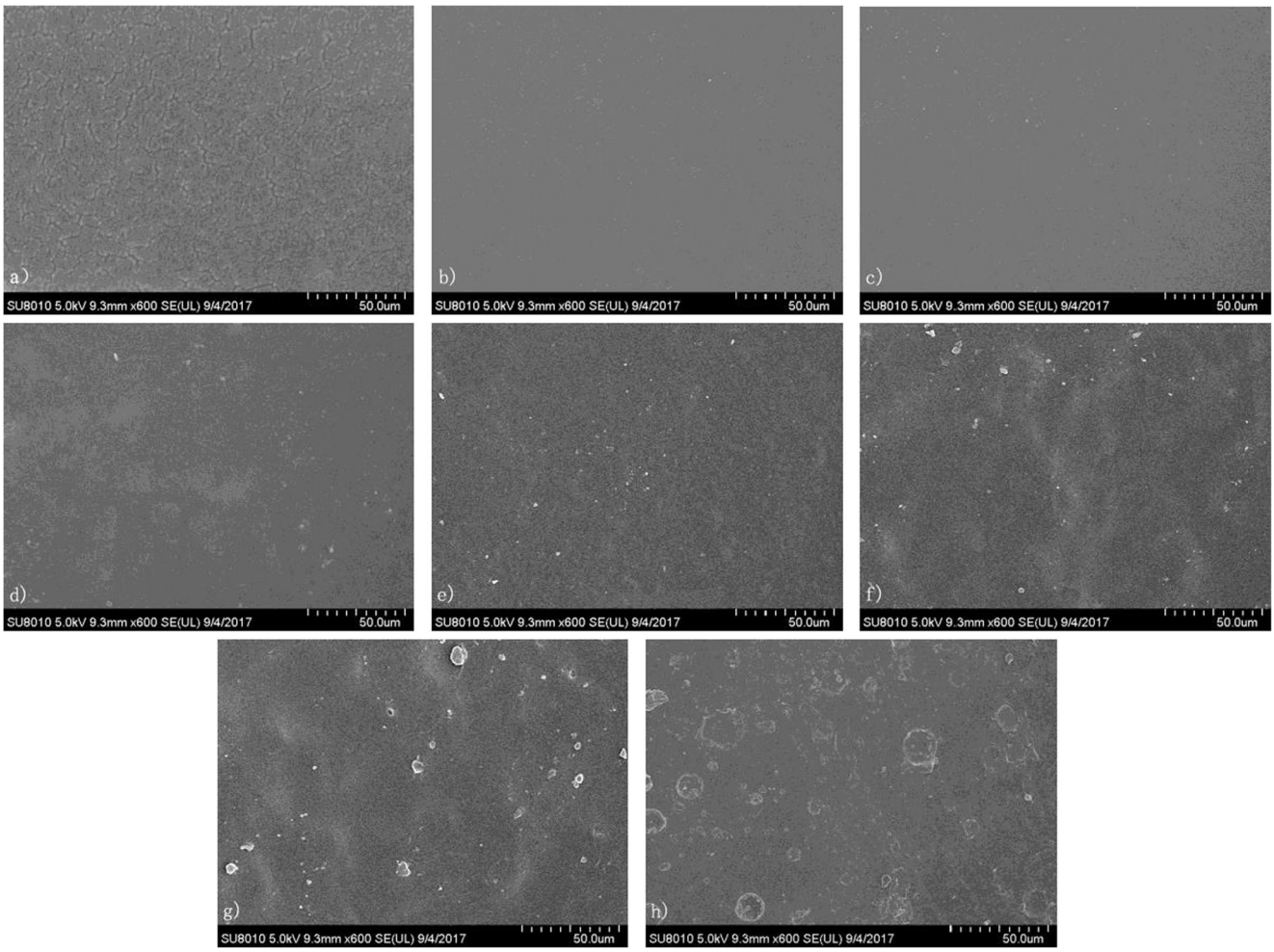

Fig. 8 Representative upper surface morphologies of composite films of **a**) PUC-0, **b**) PUC-5, **c**) PUC-10, **d**) PUC-15, **e**) PUC-20, **f**) PUC-25, **g**) PUC-30, and **h**) PUC-35

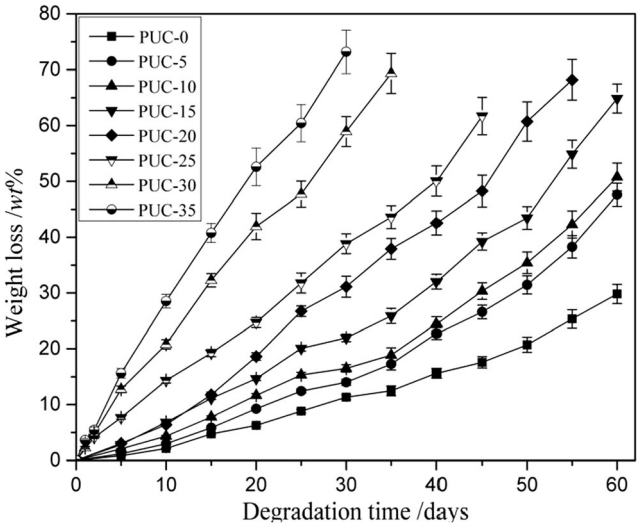

Fig. 9 Weight loss rate of composite films with different CHO content in PBS (pH: 7.4) during degradation at 37 ± 0.1 °C

pure polyurethane (PUC-0, Fig. 8a) exhibited a slightly rough surface, which should be due to the immiscibility of soft and hard segments, that is, microphase separation. When the CHO content increased from 0 to 15 *wt%* (Fig. 8a–d), the surface became much smooth. The CHO had low molecular weight and could disperse into the interspaces between soft and hard domains of polyurethane, leading to an unapparent microphase separation and smooth surface. This result was consistent with the study of DSC analysis that there was only one broad melting endothermic peak in DSC curves of the composites. While there were more and more granules observed in the surface with the CHO content increasing from 20 to 35 *wt%* (Fig. 8e–h), which may be attributed to the self-aggregation of overmuch CHO, resulting in a relatively rough film surface. Thus, in order to obtain the homogeneous-dispersed composites, the appropriate proportion of CHO in PUC was no more than 20 *wt%*, which was almost the same with the results for the mechanical property analysis.

In vitro degradation

In vitro degradation was measured via the weight loss, and the weight loss rate of composite films in PBS solution at 37 °C is shown in Fig. 9. The pure polyurethane (PUC-0) exhibited a slow degradation rate with only 28% weight loss after 60 days. It was obvious that the degradation was mainly caused by hydrolysis of ester groups. The low surface and bulk hydrophilicity of PUC-0 hindered water molecules to get close to the ester groups, resulting in slow hydrolysis rate. As it was expected, blending of polyurethane with CHO could increase the degradation rate. With the increasing content of CHO in composites (PUC-5 ~ PUC-35), the degradation rate increased gradually. The water-soluble CHO component was eluted from the composites during the incubation in PBS, which additionally facilitated the diffusion of water molecules into spaces of polymer chains that acted as a plasticizer and make the material more ductile. And then, it was easy for chain scission to take place through hydrolysis of ester bonds [34]. The results indicated that the degradation time of composite films could be controlled by adjusting the CHO content in PUC. Morphological changes in film surface directly reflected the degradation process. Fig. 10 shows the typical surface morphologies of PUC-15 after various degradation periods (predegradation and 20, 30, 45 and 60 days' postdegradation).

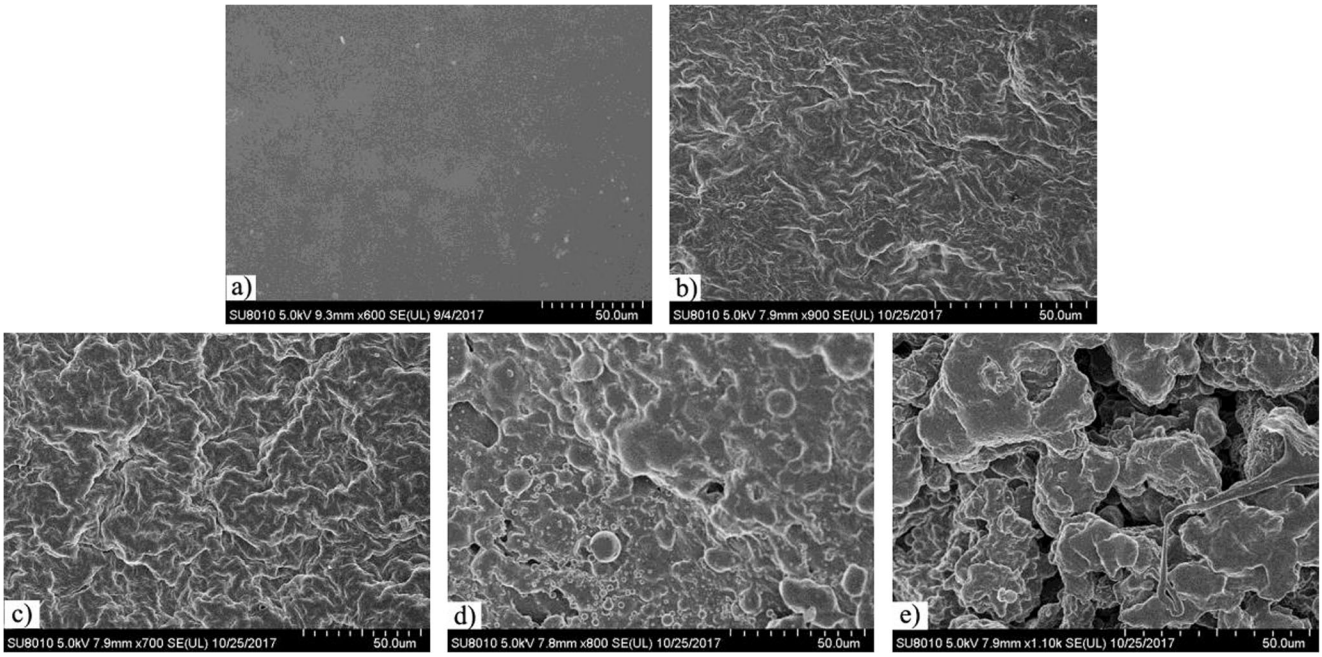

Fig. 10 Surface morphologies of PUC-15 film in PBS (pH: 7.4) at 37 ± 0.1 °C after **a**) 0, **b**) 20, **c**) 30, **d**) 45, and **e**) 60 days' degradation

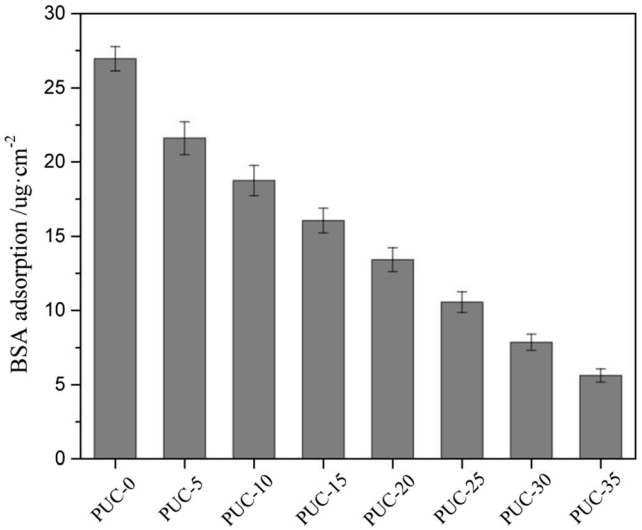

Fig. 11 The amount of BSA adsorbed on the surface of composite films with different CHO content at 37 ± 0.5 °C

The non-degraded film (Fig. 10a) was semitransparent and exhibited a smooth surface. After 20 and 30 days of degradation (Fig. 10b, c), the film surface became rougher and rougher, and then turned into some irregular hollows at 40 days (Fig. 10c). Many cracks were observed after 60 days of degradation (Fig. 10d), implying that the film gradually loses its mechanical properties.

Protein adsorption

The protein adsorption on biomaterials' surfaces is always considered as the first step to evaluate the biocompatibility (especially blood compatibility) of biomaterials [35, 36]. Figure 11 exhibits the amount of BSA adsorbed onto the surface of the composite films. As shown in the figure, when the CHO content in PUC increased from 0 to 35 *wt%*, the adsorbed amount of total protein on the surface decreased gradually from 26.9 to 5.6 μg/cm^2. This may be attributed to the blending CHO resulting in the transition from a hydrophobic surface to a hydrophilic surface. As investigated [37–40], the decrease in protein adsorption was associated with the increment in water affinity of the surfaces. The hydrophilic

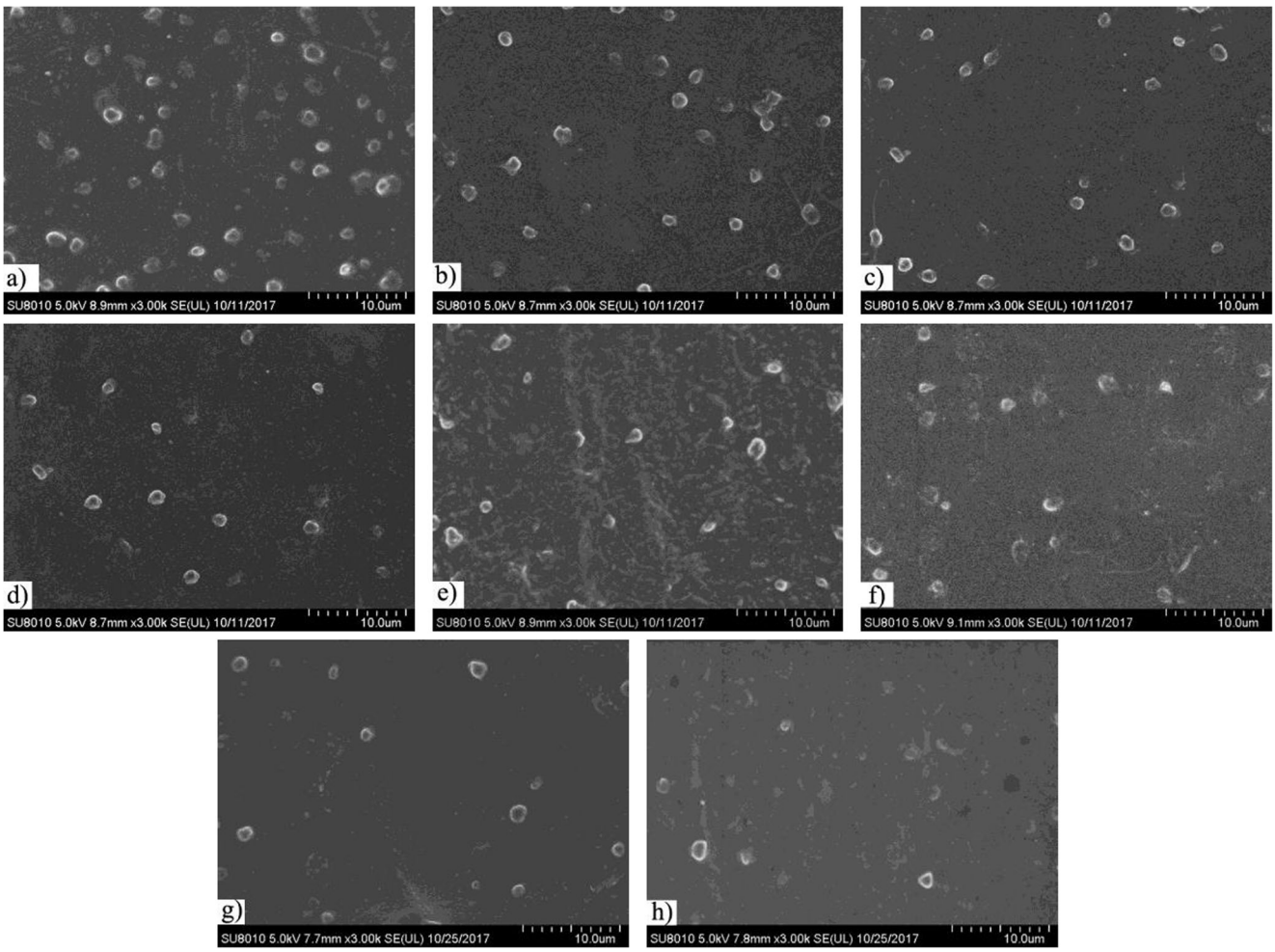

Fig. 12 Representative FE-SEM images of platelet adhesion on the surface of **a**) PUC-0, **b**) PUC-5, **c**) PUC-10, **d**) PUC-15, **e**) PUC-20, **f**) PUC-25, **g**) PUC-30, and **h**) PUC-35 films

surface could bind a significant amount of water on the surface and reduce the interaction with protein, leading to a strong repulsive force to protein. The results clearly demonstrated that surfaces with high hydrophilicity exhibited reduced protein absorption. The lower protein adsorption capacity of PEEU/CHO composite films indicated that they had higher blood compatibility than pure polyurethane films.

Platelet adhesion

Platelet adhesion on the film surface is another important test for evaluation of the blood compatibility of the blood-contacting materials. The platelet adhesion to the surface of the composite films was examined by FE-SEM, and the representative micrographs are exhibited in Fig. 12. For the pure polyurethane film (PUC-0, Fig. 12a), there were massive platelets adhering and aggregation to some extent on the surface, presenting the highly activated state. With CHO content in PUC increasing from 5 to 35 *wt%* (Fig. 12b–h), the amount of platelet adhesion on the surface decreased gradually comparing with the pure polyurethane, which proved a better anti-platelet adhesion surface. The result was in agreement with the trend of protein adsorption. One possible explanation for the good anti-platelet adhesion is that the low interfacial energy of plasma proteins on the hydrophilic surface of composite films suppresses platelet adhesion [8, 41–43]. The purpose of the work presented here is a preliminary investigation of the adhesive properties of platelets on the film surface, so the PRP used here is anticoagulated with sodium citrate which has no effect on the platelet adhesion. In-depth work will be conducted in the future, such as using human whole blood with reduced anticoagulant dose or without anticoagulants to determine the blood compatibility.

Conclusions

In this work, the novel composites of biodegradable PEEU and water-soluble CHO were prepared by a simple physical mixing, and the corresponding films were obtained by the solvent evaporation method. The influence of CHO content on the physicochemical properties of the composite films was researched. The thermal stability studies indicated that the composite films had lower initial decomposition temperature and higher maximum decomposition temperature than PEEU film. Only one broad endothermic peak found in DSC curves demonstrated the high compatibility of CHO with hard segments of PEEU. The surface morphologies of composite films indicated that the homogeneous-dispersed composites could be obtained with CHO content being less than 20 *wt%*. The ultimate stress and elongation at break of composite films decreased with the increment of CHO content, and in order to maintain the mechanical properties, the CHO content in the composites should be controlled no more than 25 *wt%*. The results of water contact angle and water absorption showed that the composite films possessed higher surface and bulk hydrophilicity which were closely related with water-solubility of CHO component. In vitro degradation studies showed that the degradation rate increased with the increment of CHO content in composites, indicating that the degradation rate of composite films could be controlled by adjusting CHO content. In addition, the surface blood compatibility of the composite films was examined by protein adsorption and platelet adhesion tests, and the results demonstrated that the composite films had improved resistance to protein adsorption and possessed excellent resistance to platelet adhesion, that is, good surface blood compatibility.

Acknowledgments This work was financially supported by Shandong Provincial Natural Science Foundation, China (ZR2018MEM024), National Undergraduate Training Programs for Innovation and Entrepreneurship, China (No. 201810445155) and Scientific Research Fund Project of Undergraduates, Shandong Normal University (No. 2018BKSKYJJ53).

References

1. Spaans CJ, Belgraver VW, Rienstra O, de Groot JH, Veth RP, Pennings AJ (2000). Biomaterials 21:2453–2460
2. Heijkants RGJC, Calck RVV, Groot JHD, Schouten AJ, van Tienen TG, Ramrattan N, Buma P, Veth RP (2004). J Mater Sci Mater Med 15:423–427
3. He W, Hu ZJ, Xu AW, Liu R, Yin H, Wang J, Wang S (2013). Cell Biochem Biophys 66:855–866
4. Shen Z, Kang C, Chen J, Ye D, Qiu S, Guo S, Zhu Y (2013). J Biomater Appl 28:607–616
5. Bochyńska AI, Hammink G, Grijpma DW, Buma P (2016). J Mater Sci Mater Med 27:85–102
6. Li D, Chen H, Glenn MW, Brash JL (2009). Acta Biomater 5: 1864–1871
7. Leckband D, Sheth S, Halperin A (1999). J Biomater Sci Polym Ed 10:1125–1147
8. Ren Z, Chen G, Wei Z, Sang L, Qi M (2013). J Appl Polym Sci 127:308–315
9. Wang DA, Ji J, Sun YH, Shen JC, Feng LX, Elisseeff JH (2002). Biomacromolecules 3:1286–1295
10. Pan Z, Hao H, Zhao Y, Li J, Tan H, Fu Q (2015). Colloid Surface B 128:36–43
11. Zhang Q, Liao JF, Shi XH, Qiu YG, Chen HJ (2015). J Polym Res 22:68–79
12. Liu H, Zhang L (2004). Polymer 45:3535–3545
13. Yu SH, Mi FL, Shyu SS, Tsai CH, Peng CK, Lai JY (2006). J Membrane Sci 276:68–80
14. Mohamed NA, Salama HE, Sabaa MW, Saad GR (2016). J Therm Anal Calorim 125:163–173
15. Mohammedi Z (2017). Int J Bioorg Chem 2:102–106
16. Usman A, Zia KM, Zuber M, Tabasum S, Rehman S, Zia F (2016). Int J Biol Macromol 86:630–645
17. Pandey AR, Singh US, Momin M, Bhavsar C (2017). J Polym Res 24:125–146
18. Zuo DY, Wang Y, Xu WL, Liu HT (2012). Adv Polym Tech 31: 310–318

19. Lin YH, Chou NK, Wu WJ, Hsu SH, Whu SW, Ho GH, Tsai CL, Wang SS, Chu SH, Hsieh KH (2010). J Appl Polym Sci 104:2683–2689
20. Chae SY, Jang MK, Nah JW (2005). J Control Release 102:383–394
21. Xu Q, Wang W, Yang W, Du Y, Song L (2017). Int J Biol Macromol 98:502–505
22. Qin C, Du Y, Xiao L, Li Z, Gao X (2002). Int J Biol Macromol 31: 111–117
23. No HK, Park NY, Lee SH, Meyers SP (2002). Int J Food Microbiol 67:65–72
24. Je JY, Park PJ, Kim SK (2004). Food Chem Toxicol 42:381–387
25. Qu WQ, Xia YR, Jiang LJ, Zhang LW, Hou ZS (2016). Chin Chem Lett 27:135–138
26. Yin S, Xia Y, Jia Q, Hou Z, Zhang N (2017). J Biomater Sci Polym Ed 28:119–138
27. Jia Q, Xia Y, Yin S, Hou Z, Wu R (2017). Int J Polym Mater Po 66: 388–397
28. Hasirci N, Aksoy EA (2007). High Perform Polym 19:621–637
29. Hou Z, Zhang H, Qu W, Xu Z, Han Z (2016). Int J Polym Mater Po 65:947–956
30. Xu W, Xiao M, Yuan L, Zhang J, Hou Z (2018). Polymers 10:580
31. Barikani M, Honarkar H, Barikani M (2009). J Appl Polym Sci 112:3157–3165
32. Li X, Liu B, Wang X, Han Y, Su H, Zeng X, Sun R (2012). J Macromol Sci A 49:861–868
33. West JC, Cooper SL (1978) Thermoplastic elastomers. In: Eirich FR (ed) Science & technology of rubber. Academic press, New York, pp 531–567
34. Brzeska J, Morawska M, Heimowska A, Sikorska W, Tercjak A, Kowalczuk M, Rutkowska M (2017). Polimery-W 62:567–575
35. Horbett TA, Brash JH (1995) Proteins at interfaces II: fundamentals and applications, in: ACS Symposium Series, vol 602. American Chemical Society, Washington
36. Seo JH, Matsuno R, Konno T, Takai M, Ishihara K (2008). Biomaterials 29:1367–1376
37. Zhang Z, Chen S, Chang Y, Jiang S (2006). J Phys Chem B 110: 10799–10804
38. Xu D, Wu K, Zhang Q, Hu H, Xi K, Chen Q, Yu X, Chen J, Jia X (2010). Polymer 51:1926–1933
39. Tangpasuthadol V, Pongchaisirikul N, Hoven VP (2003). Carbohyd Res 338:937–942
40. Liu X, Xia Y, Liu L, Zhang D, Hou Z (2018). J Biomater Appl 32: 1329–1342
41. Higuchi A, Sugiyama K, Yoon BO, Sakurai M, Hara M, Sumita M, Sugawara S, Shirai T (2003). Biomaterials 24:3235–3245
42. Lee JH, Ju YM, Kim DM (2000). Biomaterials 21:683–691
43. Milner KR, Snyder AJ, Siedlecki CA (2006). J Biomed Mater Res A 76:561–570